$$x/d/(M^2C_D^{1/2}) = (\pi/8b)^{1/2}\tau, \quad r/d/(MC_D^{1/2}) = (\pi/8b)^{1/2}\lambda \quad (5)$$

Thus, the complete steady flow pattern can be obtained from the unsteady cylindrical wave pattern.

In the far-field (weak shock region), since the overpressure of the positive phase varies linearly with the space variables, the positive phase overpressure, which has practical importance, can be described by the shock overpressure $(\Delta p/p_o)_s$, the shock position $x_s$ vs $r_s$, and the duration $L_r$ (in the radial direction) or $L_x$ (in the axial direction) of the positive phase signature. The explicit and useful relations can be readily obtained from Eqs. (1–3): the shock position,

$$\frac{x_s/d}{M^2C_D^{1/2}} = \frac{r_s/d}{MC_D^{1/2}} - 0.101 - 0.416\left[\frac{(r_s/d)^{1/2}}{M^{1/2}C_D^{1/4}} - 0.721\right]^{1/2} \quad (6)$$

the shock overpressure

$$\left(\frac{\Delta p}{p_o}\right)_s = 0.306\,\frac{MC_D^{1/2}}{r_s/d}\left[\frac{(r_s/d)^{1/2}}{M^{1/2}C_D^{1/4}} - 0.721\right]^{-1/2} \quad (7)$$

and the durations of the positive phase

$$\frac{L_x/d}{M^2C_D^{1/2}} = \frac{L_r/d}{MC_D^{1/2}} = 0.416\left[\frac{(r_s/d)^{1/2}}{M^{1/2}C_D^{1/4}} - 0.721\right]^{1/2} \quad (8)$$

The extrapolation expressions, Eqs. (6–8), and the original Plooster's numerical data valid in the near field of the hypersonic body are plotted in Fig. 1.

## Conclusions

An approximate method is developed for determining the far-field flow pattern of hypersonic bodies. For our special interests on sonic booms, the sonic boom shock overpressure, locations and the positive phase duration are expressed explicitly in terms of the Mach number, drag coefficient, and dimension of hypersonic vehicles.

Numerical examples have been carried out and reported in Ref. 4 for several steady level flights and for a typical glide trajectory of space shuttles. Figure 2 shows the sonic boom positive phase signatures of a hypersonic vehicle during its steady level flights. $C_D = 0.914$ at several altitudes and Mach numbers are assumed. The general behavior of the sonic boom during steady level flights is consistent with that of the sonic boom of supersonic vehicles. That is the larger the Mach number, the larger the drag coefficient, or the lower the altitude, the larger are the sonic boom overpressure, positive duration, and sonic boom impact. For a typical glide trajector of space shuttles, approximate results indicate that the sonic boom may be felt along the ground trace of space shuttles.

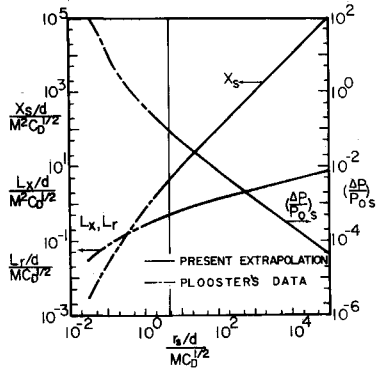


**Fig. 1 Sonic boom overpressure $(\Delta p/p_o)_s$, position $x_s$, and positive phase duration $L_r$ or $L_x$ vs shock radius $r_s$.**

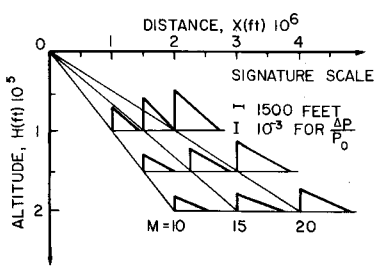


**Fig. 2 Sonic boom positive phase signatures ($C_D = 0.914$).**

### References


[1] Miller, D. S., Morris, D. A., and Carlson, H. W., "Wind-Tunnel Investigation of Somic-Boom Characteristics of Two Simple Wing Models at Mach Number from 2.3 to 4.63," TN D-6201, April 1971, NASA.

[2] Hayes, W. D. and Probstein, R. F., *Hypersonic Flow Theory*, Vol. 1, 2nd ed., Academic Press, New York, 1966, Chap. I and II.

[3] Lin, S. C., "Cylindrical Shock Waves Produced by Instantaneous Energy Release," *Journal of Applied Physics*, Vol. 25, 1957, pp. 54–57.

[4] Pan, Y. S. and Sotomayer, W. A., "Far-Field of a Hypersonic Body," to be presented at the Sixth Southeastern Conference on Theoretical and Applied Mechanics, Univ. of South Florida, Tampa, Fla., March 23–24, 1972.

[5] Whitham, G. B., "On the Propagation of Weak Shock Waves," *Journal of Fluid Mechanics*, Vol. 1, Pt. 3, 1956, pp. 290–318.

[6] Plooster, M. N., "Shock Wave from Line Sources. Numerical Solutions and Experimental," *The Physics of Fluids*, Vol. 13, No. 11, 1970, pp. 2665–2675.

[7] Plooster, M. N., "Erratum: Shock Waves from Line Sources. Numerical Solutions and Experimental Measurements," *The Physics of Fluids*, Vol. 14, No. 10, 1971, p. 2248.


# Structural Optimization in Random Vibration Environment


N. C. NIGAM*

*Indian Institute of Technology, Kanpur, India*


### Introduction

ALL flight vehicles operate in random vibration environment. A realistic formulation of the optimum design problem for flight vehicle structures must, therefore, contain probabilitsic constraints on the dynamic response of the system. In this note the optimization problem in random vibration environment is stated and transformed to a standard nonlinear programming problem. Two simple examples with weight and expected rate of fatigue damage as objective functions are presented to illustrate the application of the proposed formulation.

### Optimization Problem

A typical optimization problem in random vibration environment can be stated as: Minimize

$$W(\bar{D}) \quad (1)$$

subject to

$$P\left[\bigcup_{\substack{i=1 \\ a\le t\le b}}^{k}\left\{s_i(\bar{x}(\bar{D},t)) \ge r_i\right\}\right]_j \le [p_f]_j \qquad j = 1, 2, \ldots, m \quad (2)$$

$$s_j(\bar{D}) \le r_j \qquad j = m+1, \ldots, n \quad (3)$$

and

$$f_i^{(l)} \le f_i \le f_i^{(u)} \qquad i = 1, 2, \ldots, p \quad (4)$$

where $W(\bar{D})$ is the objective function, $\bar{D}$ is the vector of the design variables, $\bar{x}(\bar{D}, t)$ represents the dynamic response of the system, $s_i[\bar{x}(\bar{D}, t)]$ is a response function, $r_i$ is a deterministic or random constraint on $s_i$, $[p_f]_j$ denotes the specified upper bound on the probability of failure in mode $j$, $f_i$ is the $i$th natural frequency of the system and $f_i^{(l)}$ and $f_i^{(u)}$ denote the lower and upper bounds on the frequency.

The dynamic response of a large class of problems can be treated as a stationary random process. In such cases the mean

Received November 4, 1971.

* Assistant Professor, Aeronautical Engineering Department.

and the variance of the response are independent of time, and where probability estimates can be made in terms of these functions, time dependence can be eliminated from inequality (2). Let $S_i(\bar{x}(\bar{D}, t)]$ be a stationary random process and let

$$P[s_i(\bar{x}(\bar{D}, t)) \geq r_i] = q_i(\bar{D}) \qquad (5)$$
$$\infty < t < \infty$$

then

$$P\left[\bigcup_{\substack{i=1 \\ -\infty<t<\infty}}^{k} \left\{ s_i(\bar{x}(\bar{D}, t)) \geq r_i \right\}\right] \simeq \sum_{i=1}^{k} q_i(\bar{D}) \text{ if } q_i \ll 1 \qquad (6)$$

Inequality (2) can now be replaced by

$$\left[\sum_{i=1}^{k} q_i(\bar{D})\right]_j = h_j(\bar{D}) \leq [p_f]_j \qquad j = 1, 2, \ldots, m \qquad (7)$$

In particular, if $S$ and $R$ are normal and statistically independent

$$q(\bar{D}) = \frac{1}{(2\pi)^{1/2}} \int_{\mu_R - \mu_S/(\sigma_S^2 + \sigma_R^2)^{1/2}}^{\infty} e^{u^2/2}\, du \qquad (8)$$

where $\mu_R$, $\mu_S$ and $\sigma_R$, $\sigma_S$ are mean and standard deviation of $R$ and $S$, respectively. Note that Eq. (8) requires only the mean and the variance of $S$ and $R$. In problems where exact estimates of $q_i$ cannot be obtained, the left hand side of inequality (2) may be replaced by its upper bound estimate.[1] Nonstationary response problems can also be treated in this manner.

With inequality (2) replaced by inequality (7), the optimization problem is reduced to minimization of $W(\bar{D})$ subject to inequality constraints (3), (4) and (7). In this form the optimization problem is a standard nonlinear programming problem which can be solved by any of the well known methods.

1) Two Bar Truss—A two bar truss, shown as inset in Fig. 1,

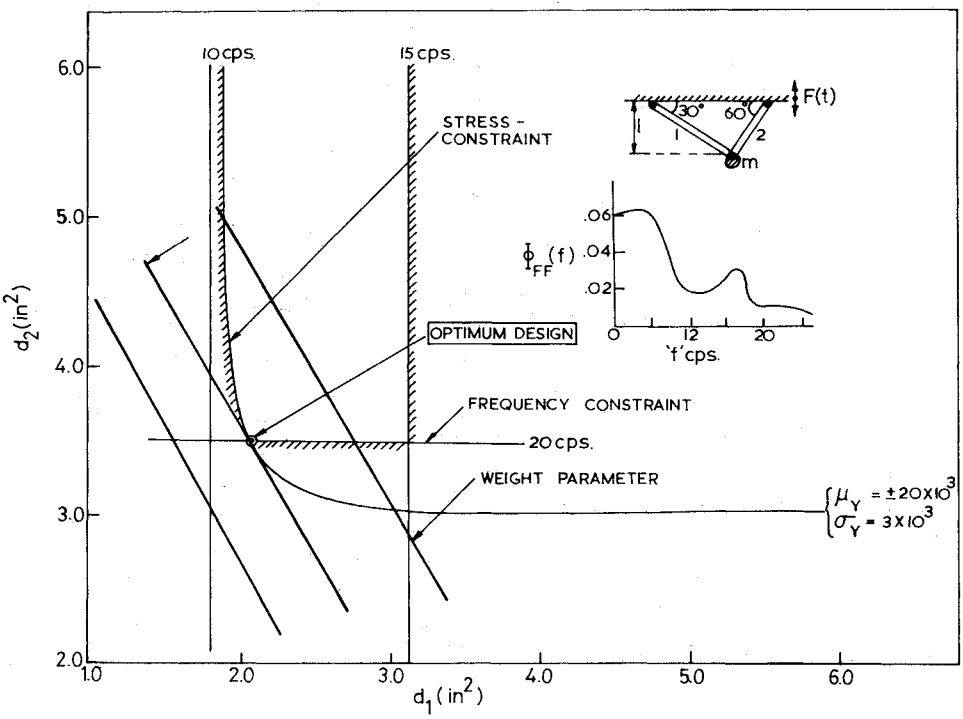


**Fig. 1 Two bar truss.**

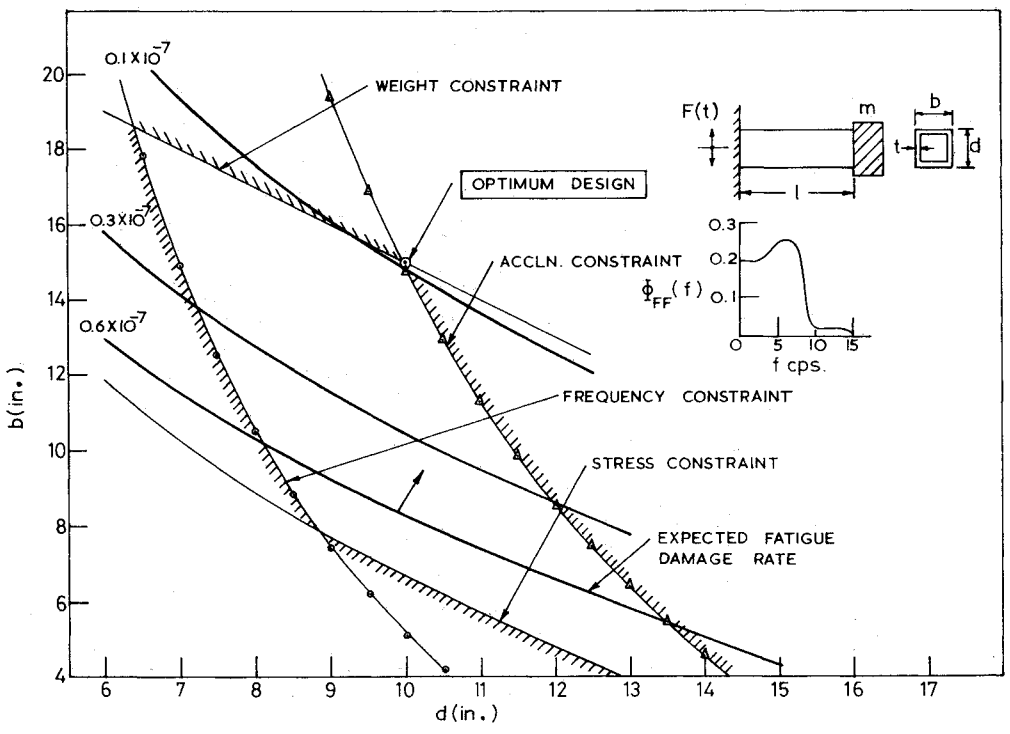


**Fig. 2 Cantilever with tip mass.**

is subjected to base acceleration $F(t)$ having a zero mean and power spectral density (PSD) $\phi_{FF}(f)$ shown in Fig. 1. The optimization problem is stated as: Minimize-Weight Function:

$$W(\bar{D}) = \rho(d_1 l_1 + d_2 l_2)$$

subject to stress constraint

$$P\left[\bigcup_{\substack{i=1 \\ -\infty<t<\infty}}^{2} \left\{|s_i(t)| \geq r\right\}\right] \leq 10^{-3}$$

Frequency constraint

$$10 \leq f_1 \leq 15, \qquad f_2 \geq 20$$

where $s_i$, $i = 1, 2$ is stress in the $i$th bar, $r$ is the random yield stress with mean $\mu_R = \pm 20 \times 10^3$ psi and standard deviation $\sigma_R = 3 \times 10^3$ psi. $F(t)$ and $Y$ are assumed to be independent and Gaussian. Mean and Variance of the stresses is obtained using the frequency domain approach. Since the problem has only two design variables, optimum design is obtained graphically as shown in Fig. 1.

Note that the frequency constraint is specified such that the natural frequencies of the system lie in regions where $\phi_{FF}(f)$ has small values and is flat. This has the effect of reducing the response and thereby leading to a better design. Also since the spectral density is flat in the region of interest, calculations can be simplified by the white noise assumption for lightly damped structures.[2]

2) Cantilever with Tip Mass—A cantilever beam with thin-walled box section and a tip mass, shown as inset in Fig. 2, is subjected to a base acceleration $F(t)$ with zero mean and PSD $\phi_{FF}(f)$ as shown in Fig. 2. The optimization problem is stated as: Minimize—Expected Rate of Fatigue Damage[2]

$$ED(\bar{D}) = \frac{N_0^+}{\beta}[(2)^{1/2}\sigma_S]^{\alpha}\Gamma(1 + \alpha/2)$$

subject to stress constraint

$$P\underset{-\infty<t<\infty}{}[|s(t)| \geq r] \leq 10^{-3}$$

acceleration constraint

$$P\underset{-\infty<t<\infty}{}[|a(t)| \geq 10g] \leq 10^{-3}$$

weight constraint

$$W/\rho l \leq 10$$

frequency constraint

$$f \geq 10$$

where $N_o^+$ is the number of zero crossings with positive slope, $\alpha = 6.0$, $\beta = 6.4 \times 10^{31}$ are coefficients in the assumed law of fatigue failure ($Ns^{\alpha} = \beta$), $s$ is the maximum stress at the root of the cantilever, $r$ is the yield stress with mean $\mu_R = \pm 18 \times 10^3$ psi and $\sigma_R = 2 \times 10^3$ psi, $a$ is the absolute acceleration of the tip mass, $W$ is the weight of the beam, and $f$ is the fundamental frequency of the system in cps. Response calculations have been carried in the frequency domain assuming the beam to be weightless. Thickness of the beam was assumed to be constant and equal to $t = 0.2$ in., tip mass $m = 1.0$ and viscous damping $\zeta = 0.02$. Since thickness is assumed to be constant, the problem has two design variables, width $b$ and depth $d$. Graphical solution (Fig. 2) gives the optimum design: $b = 15$ in., $d = 10$ in. and $t = 0.2$ in. with objective function $ED = 1.0 \times 10^{-8}$.

The problem was also solved for three design variables $b$, $d$, $t$ using unconstrained minimization technique. The optimum design is obtained for $b = 36.62$ in., $d = 9.2$ in. and $t = 0.108$ in. with $ED = 0.645 \times 10^{-8}$, giving a reduction of 35.5% over previous design.

### Conclusions

The optimization problem with probabilistic constraints on the dynamic response of a system can be transformed to a standard nonlinear programming problem and solved by any of the well-known methods. Constraints on the natural frequencies of the system are both important and convenient in such problems. Power spectral density curves provide a direct visual basis for choosing these constraints.

### References

[1] Shinozuka, M., "Probability of Structural Failure Under Random Loading," *Engineering Mechanics Division Journal*, ASCE, Vol. 90 (EM5), 1964, pp. 147–170.

[2] Lin, Y. K., *Probabilistic Theory of Structural Dynamics*, 1st ed. McGraw-Hill, New York, 1967, chaps. 5 and 9.

# Effects of Transverse Outflow from a Hypersonic Separated Region

ALLEN H. WHITEHEAD JR.,* JAMES R. STERRETT,‡ AND JAMES C. EMERY‡

*NASA Langley Research Center, Hampton, Va.*

THE design of hypersonic configurations such as the space-shuttle must consider the consequences of separated flows over protrusions, control surfaces or ahead of jet-interaction controls. These flows will be characterized by transverse-relief effects. Particularly in the critical region around reattachment where the pressure and heating are experimentally and theoretically important, data are extremely limited, and no hypersonic studies can be found to indicate the effect of a systematic variation in transverse outflow on conditions at the reattachment point even over nominally two-dimensional geometries. Recent reviews of the separation problem (for example, Ref. 1) recognize that the pressure rise at reattachment provides a closure condition in the analysis which is as important as the separation point and the separated shear layer in determining the structure and properties of the separated flow region. Most theoretical models do not account for transverse outflow effects, but assume as in the Chapman[2] approach that fluid escapes the separated region only through mixing across the separated shear layer. The present study examines features of hypersonic, finite-span separated flows with a turbulent boundary-layer to provide a partial assessment of transverse-outflow effects on separated flowfield characteristics.

An illustration of three-dimensional separated flows is given in Fig. 1 which shows an unpublished oil flow photograph of the canopy region of a straight-wing shuttle orbiter (from an investigation reported in Ref. 3). A clearly identified reattachment occurs as well as extensive transverse flow from the reverse-flow region. Other regions on this orbiter also exhibit three-dimensional separation. To provide a preliminary assessment of such outflow effects, studies were conducted on variable-span, forward-facing steps and wedges ($\bar{w}$ = ratio of model span to full-span step or wedge) in the Langley 20-in. Mach 6 Tunnel at a unit Reynolds number of 21 million/m (6.4 million/ft). The span of the plate was 25 cm, and the distance from the leading edge to the step or wedge was 39.4 cm. The constant step height of 2.92 cm ($h$) was about five times the boundary-layer thickness just upstream of separation; the 40° wedges had a slant length ($h$) of 10.6 cm. From criteria developed by Morrisette et al.,[4] roughness elements placed 5.0 cm from the plate leading edge assured a well developed turbulent boundary-layer prior to separation. Oil flow studies were used to locate separation and reattachment.

Received November 15, 1971.

* Aerospace Engineer, Configuration Flow Fields Section. Associate AIAA.

† Head, Configuration Flow Fields Section. Member AIAA.

‡ Aerospace Engineer, Configuration Flow Fields Section.